OPTICAL CHARACTERISTICS OF THE WHIPPLE OBSERVATORY TEV GAMMA-RAY IMAGING TELESCOPE

D. A. LEWIS
Physics Department, Iowa State University, Ames, Iowa 50011

(Received 9 May, 1989; accepted 18 April, 1990)

Abstract. In TeV γ-ray astronomy, large mirrors are used to collect Čerenkov light from electromagnetic cascades in the atmosphere in order to obtain low energy thresholds. The flux sensitivity of TeV γ-ray detectors is limited by background due to Čerenkov light bursts from isotropic, cosmic-ray showers which are much more numerous than γ-ray showers. It has recently been established that most of this background can be eliminated on the basis of the shapes of Čerenkov light images on the focal plane of a telescope. In order for this technique to work, the light collector must have adequate resolution over a relatively wide field of view. In this paper, the optical characteristics of the 10 m reflector used in the imaging detection of the Crab Nebula are examined and contrasted with those of a standard parabolic design. This 10 m reflector has a unique (Davies-Cotton) design with small spherical facet mirrors placed on spherical support structure with radius equal to exactly 1/2 the curvature radius of the facet mirrors. The off-axis focusing properties of this type of telescope have not been examined previously.

Keywords : instrumentation, observation methods.

1. Introduction

The atmospheric Čerenkov technique has become an established method for detecting cosmic sources of 10^{12} eV (TeV) γ-rays (Weekes 1988). At TeV energies, a primary photon striking the atmosphere gives rise to a cascade of highly relativistic electrons, positrons, and secondary γ-rays via pair production and bremsstrahlung. Although few of the charged particles reach ground level at the 2320 m altitude of Whipple Observatory at TeV energies, Čerenkov light from relativistic charged secondaries acts as a penetrating component which does reach ground. Because the charged particles, γ-rays, and Čerenkov photons all travel at nearly c, the Čerenkov light arrives in a short burst, only a few ns wide. This short time correlation makes it possible to unambiguously detect Čerenkov light against a much larger background of Poisson-fluctuating night sky light. Basically only a large reflector and a photomultiplier tube with fast electronics are needed. A major advantage of the technique is that light from a single primary γ-ray is spread over a circular area approximately 200 m in diameter by the time it reaches ground level, giving a telescope an effective aperture of 200 m. The physical aperture of the telescope determines an effective threshold above which γ-rays are detected.

Although it is possible to detect cosmic-ray showers with relatively simple equipment, definitive observations to characterize (or even convincingly demonstrate the existence of) cosmic γ-ray sources are difficult because of the large background of

Experimental Astronomy **1**: 213–226, 1990.

isotropic very high energy protons striking the earth's atmosphere. These cosmic-ray protons initiate showers with properties similar (but not identical) to those of γ-ray showers. This has led to methods to discriminate γ-ray showers from proton showers on the basis of time-width of the Čerenkov light pulse (Fegan et al. 1968, Resvanis et al. 1986), UV content of the light (Stepanian et al. 1983), and angular distribution of the light (Weekes and Turver 1977, Hillas 1985, Cawley et al. 1985). For general reviews of techniques see, e.g., Fry (1986), or Weekes (1988).

Recently the Whipple Observatory collaboration has detected a flux of about $7 \cdot 10^{-11}$ photons/(cm^2-s) above a threshold of 0.4 TeV from the Crab Nebula at the 15σ level using the angular distribution of the Čerenkov light (i.e., the shape of the image on the focal surface of a telescope) to eliminate 98 percent of the background events (Lang et al. 1989). This detection establishes imaging as a working technique for significantly increasing the sensitivity of Čerenkov telescopes. It also suggests that the Crab Nebula is a continuous source of VHE γ-rays providing a weak but apparently steady "standard candle." As described in Sec. IV the success of the imaging technique depends on the resolution of the telescope both on and off the optic axis.

In this paper, the optical properties of the 10 m reflector at the Whipple Observatory (Cawley et al. 1990) are examined. The reflector is a tessellated structure of unusual design based upon a solar concentrator proposed and built by Davies and Cotton (1957). It consists of small, identical spherical mirrors mounted on a spherical structure whose radius of curvature is exactly 1/2 that of the individual mirrors. Although Davies and Cotton were concerned only with optimal resolution on the optic axis, it will be shown in this work that the unique design also reduces aberrations for off-axis rays as well, yielding good resolution across a 4° field of view.

The purpose of this study is threefold. The off-axis focusing properties of Davies-Cotton reflectors have not been examined previously. It is shown here that the off-axis properties are in fact superior to a standard parabolic design. Secondly, since the Čerenkov imaging technique rests upon detailed Monte Carlo simulations of the development of extensive air showers, an accurate description of the reflector optics is necessary in modeling the response of the telescope. This is provided by this work. Finally, a comparison of the Davies-Cotton design with a standard parabolic design is made in the context of Čerenkov light imaging telescopes, in preparation for the addition of a second imaging telescope to the existing one at Whipple Observatory (GRANITE, see, e.g., Akerlof 1989).

2. Basic telescope design — on-axis aberrations

The reflector used in the Whipple Observatory Čerenkov telescope is a Davies-Cotton design consisting of 248 identical mirrors, each with a 14.6 m radius of curvature, positioned in a hexagonal pattern covering a spherical bowl of radius 7.3 m with an opening diameter of 10 m. The focal plane is at the center of curvature

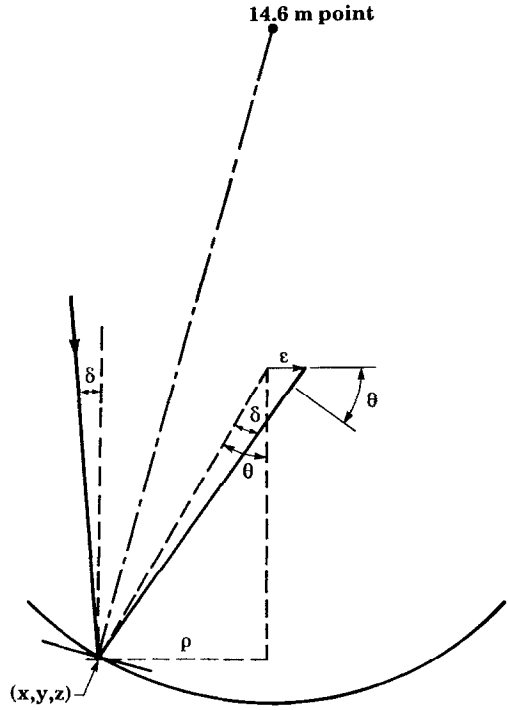

Fig. 1. The basic geometry of the telescope is shown above. The facet mirrors are pointed at the 14.6 m point along the axis of the reflector. An incoming ray making angle δ with the optic axis will appear on the focal plane displaced by ϵ.

of the 7.3 m radius bowl, making the plate scale (the linear displacement on the focal plane per angular displacement of a ray from the optic axis) 12.8 cm/degree and the reflector an $f/0.7$ system. The advantages of a Davies-Cotton design are (1) all facet mirrors are identical, (2) the alignment procedure is straightforward, (3) the overall structure of the 10 m, $f/0.7$ system is rigid and compact, and (4) as shown below, off-axis aberrations are reduced.

A disadvantage of the Davies-Cotton design for Čerenkov work is that light travel times from different portions of the mirror reach the focal plane at different times, i.e., it is not isochronous. Since the individual facets are not positioned on a paraboloid, the light travel times for photons striking outer mirrors are up to 6 ns shorter that for photons striking mirrors near the center of the reflector. Although this property is not directly related to the optical quality of the images, it is nevertheless intrinsic to the design and implies that longer integration times are necessary to capture an image. This introduces additional noise from general night-sky light, which does degrade the images in practice (Cawley et al. 1990).

Fig. 1 is a diagram of the telescope shown pointing at the zenith. A facet mirror

located at distance ρ from the optic axis is aligned so that a normal vector from its center is aimed toward a point on the optic axis 14.6 m from the telescope. All 248 facet mirrors are aligned in this way. Light from a point source at infinity striking the center of the mirror is then reflected toward the center of the image plane, 7.3 m from the reflector. This follows because (1) the center of the facet mirror, (2) the center of image plane, and (3) the 14.6 m point on the optic axis, form an isoceles triangle. The alignment procedure consists of placing an arc-lamp/telescope at the 14.6 m point on the optic axis and adjusting the pointing of each of the 248 facet mirrors to retro-reflect to the 14.6 m point.

Each facet mirror has a 14.6 m radius of curvature and functions as an off-axis spherical mirror of focal length 7.3 m. The individual mirrors are hexagons, 61 cm across, and arranged in the hexagonal pattern covering a 75 m^2 area. The front surface mirrors are coated with aluminum and overcoated with quartz. For incident rays parallel to the optic axis, the aberrations of individual mirrors have been discussed before (Ricke 1969), and are briefly reviewed here. Spherical aberration for an off-axis spherical mirror gives rise to a disk of confusion of diameter $r^3/4R^2$ where r is the radius of the mirror and R is the radius of curvature of the mirror (Smith 1966); for the 10 m reflector this is a negligible 0.026 cm (0.002°). The effect of coma is to cause the image to be roughly elliptical with maximum dimension of $3ir^2/2R$ where i is the angle (in radians) made by the incident rays with the optic axis of the mirror. It has a maximum value of 0.5 cm (0.04°) for mirrors in the outer ring, and goes to zero for the inner rings.

By far the largest aberration is astigmatism, which may be calculated as follows. An off-axis spherical mirror has a sagittal line focus and a tangential line focus with minimum disk of confusion about midway between them. The distances to these line foci are (see, e.g., Smith 1966)

$$d_{\mathrm{sag}} = R/(2\cos(i)) \qquad d_{\mathrm{tang}} = R\cos(i)/2$$

where R is the curvature radius of the mirror. For the outer ring of mirrors, i is about 0.36 radians (21°), implying the minimum confusion waist is 7.3 m + 0.02 m from the surface of the mirror. By projecting the mirror size onto the location of the disk of least confusion, its size can be shown to be 4.4 cm (0.34°) for mirrors in the outer ring, and goes to zero for the inner rings. The small focus displacement for the outer ring of mirrors (0.02 m) from 7.3 m justifies the use of identical focal lengths of 7.3 m for all individual facet mirrors.

A measured point spread function for the 10 m spherical reflector is shown in Fig. 2 for the center of the field of view. This was measured by moving the reflector while a masked photomultiplier tube recorded the light from Polaris. The estimated measurement error is 0.02° in angle and 5% in intensity. The mirrors had been aligned just before the measurements were taken. The FWHM of the measured distribution is about 0.12° and the rms width is 0.05°. Also shown in the figure is a calculated point spread function (solid line) in which the classical

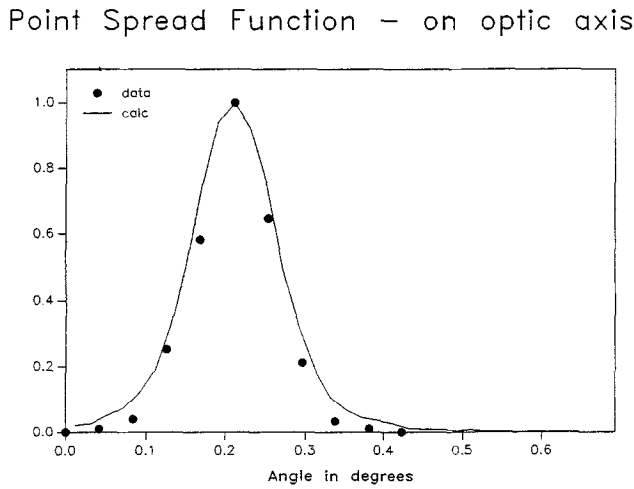

Fig. 2. A measured point spread function on the optic axis is shown. The zero of the x-axis is arbitrary and the solid curve was calculated as described in the text.

aberrations (spherical, coma, astigmatism) were all included for each facet mirror. An overall gaussian width of 0.1°, an estimate (Weekes 1988a) of pointing errors and imperfections in the mirrors, was included in the calculations for each facet mirror via Monte Carlo methods. It was assumed that a set of incoming photons uniformly illuminated the reflector and each photon was traced to the image surface. The calculated curve is normalized to match the data at the highest point. The fit could be improved with a smaller value for the pointing error estimate.

3. Off-axis aberrations

As the size of individual facets becomes arbitrarily small, the image of a point source on the optic axis also becomes arbitrarily small provided one stays within the geometrical optics limit. For a Davies-Cotton reflector, the individual facets are not tangent to the overall spherical shape but rather point toward a position on the optic axis exactly two focal lengths from the center of the reflector. Therefore the reflector does not become smooth for small facet size. This is in contrast to a normal parabolic mirror for which the facets are tangent to the overall structure and also have the same radius of curvature as the overall structure. An ideal tessellated paraboloid becomes smooth for arbitrarily small facet size.

As the source moves off the optic axis, a "global" aberration related to the overall shape of the reflector appears and quickly dominates the image shape and the aberrations of individual facet mirrors become less important. This global aberration has not been discussed or analyzed previously for a Davies-Cotton telescope. It arises because, for off-axis rays, the facet mirrors no longer point in the right direction for the rays to converge to a point. This can be seen from the diagram in Fig. 1. An incident light ray displaced from the optic axis in the plane of incidence

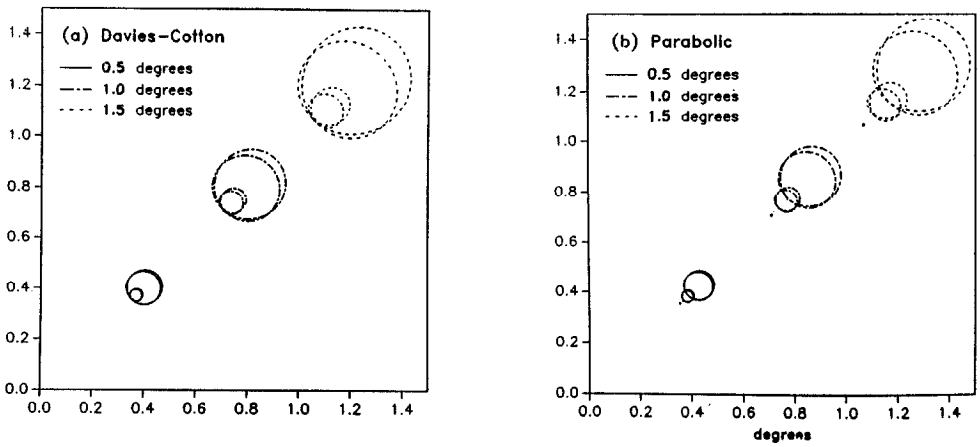

Fig. 3. Cometary circles for (a) the Whipple Observatory tessellated 10 m Davies-Cotton reflector and (b) a conventional tessellated parabolic reflector are shown above. The incident light strikes mirrors at radii of 1 m, 6 m, and 9 m from the center of reflector. In the three cases shown, it is displaced by 0.5°, 1.0°, and 1.5° from the optic axis.

by a small angle δ strikes a mirror a distance ρ from the center of the reflector. The position of the mirror could also be described as being at angle θ with respect to the optic axis, and $\rho = (7300\,\text{cm})\sin(\theta)$. For this case, it is apparent from the figure that the ray crosses the focal plane at distance $\epsilon = (7300\,\text{cm})\tan(\delta)/\cos(\theta)$ from the center of the focal surface. Now suppose that the ray were displaced by δ in a direction perpendicular to the plane of incidence striking a mirror at distance ρ from the center of the reflector but out of the plane of the figure. It would then cross the focal plane at distance $\epsilon = (7300\,\text{cm})\tan(\delta)$. By continuing the argument for rays illuminating a particular ring of mirrors on the reflector, it becomes apparent that the light forms a reentrant double (cometary) ring on the focal plane.

The cometary rings corresponding to point sources 0.5°, 1.0°, and 1.5° from the optic axis are shown in Fig. 3a for the 10 m spherical reflector and in Fig. 3b for a normal parabolic reflector. At each angle, rings of mirrors at distances of 1 m, 5 m, and 9 m from the reflector are illuminated with cylinders of light. The size of the resulting light rings in the focal plane increase rapidly with the diameter of the ring of mirrors at the reflector, and the 1 m ring focuses essentially to a point. The results in Fig. 3 were calculated using a ray-tracing program written specifically for this work, and the facet mirrors were assumed to be free of aberrations and pointing errors.

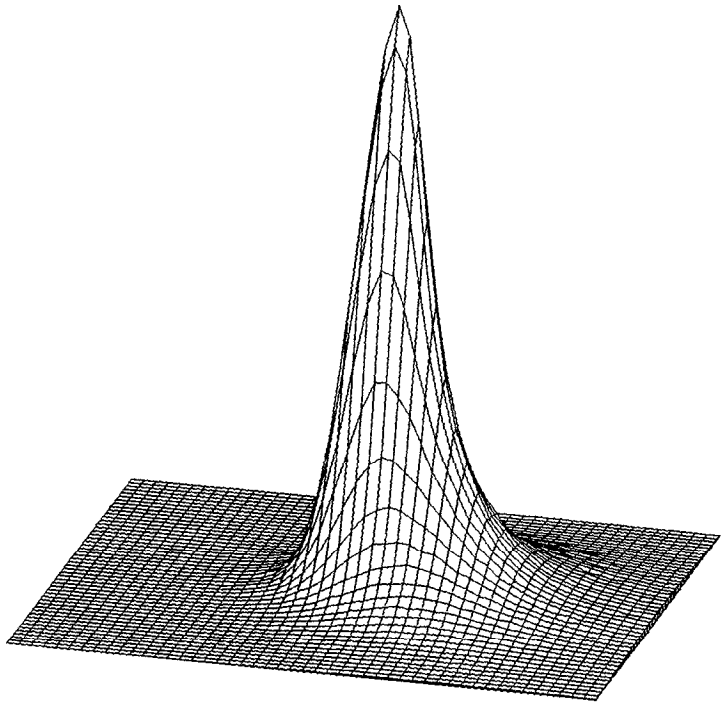

Fig. 4. The calculated image shape for point source at infinity and 1.5° from the optic axis of a Davies-Cotton reflector is shown above. The optic axis is off to the left. With no aberrations the image would be a delta-function at the center of the grid.

The rings for the parabolic design march outward for light striking mirrors further from the optic axis because the mirrors are also at increasing distances from the focal surface. Hence the usual comet-shaped patterns are found for a parabolic shape. However the rings for a Davies-Cotton reflector are all tangent to a single point (the no-aberration point) on the focal plane because the facet mirrors are all at the same distance from the focal plane. This results in a relatively sharply peaked point spread function even for off-axis rays as shown in Fig. 4. The calculated image shown in the figure is located 1.5° from the center of the field view (off to the left in the figure) and has a FWHM of about 0.15° in the radial direction and about 0.12° in the azimuthal direction. The grid lines in the figure are separated by 0.02°. With no aberrations, the image would occupy a single pixel at the center of the grid. As well as the global aberration, classical aberrations and pointing errors in the facet mirrors, were included in the calculation.

Although the FWHM of the peak 1.5° from the optic axis (Fig. 4, 0.15°) is not much wider than an on-axis peak (Fig. 2, 0.12°) a significant amount of light is lost because of rapid defocusing of light from the outer rings which is spread over

a large area. This can be quantified by plotting the fraction of light from a point source which passes through a disk of varying diameter on the focal plane of the telescope (Rieke 1969). Such an "integral image shape" plot is shown in Fig. 5a for a Davies-Cotton telescope (the existing 10 m at Whipple Observatory), and in Fig. 5b for a comparable parabolic-design telescope. The abscissa is the diameter of the disk and the ordinate is the fraction of light passing through it. The three curves for each telescope design correspond to a point source (*i*) on the optic axis, (*ii*) 1° off the optic axis, and (*iii*) 1.5° off the optic axis. The Davies-Cotton telescope has facet mirrors with constant radii of curvature of 14.6 m whereas it is assumed that each ring of the parabolic design has a radius of curvature chosen to minimize astigmatism for that ring. Facet-mirror classical aberrations and pointing errors, as well as global aberrations, were included as described above.

As can be seen from Fig. 5, the parabolic design yields slightly better light concentration at the center of the focal surface whereas the Davies-Cotton design is superior for off-axis images. The reason that the parabolic design is slightly better on axis is that the outer rings of facet mirrors are somewhat further from the focal surface. This slightly reduce astigmatism, the dominant facet aberration for the outer rings. The Davies-Cotton design yields significantly better off-axis concentration because the "global" coma due to the overall shape is reduced.

A measured point spread function for the present 10 m reflector is shown in Fig. 6 for a point 1.25° from the center of the field of view. The measurement was made (as described previously) in the radial direction and the cometary tail is clearly present. The FWHM is about 0.14°, which is comparable to the on-axis FWHM of 0.12°, however the rms width is 0.13°, which is significantly larger than the on-axis value of 0.05°. The solid curve in the figure was calculated using facet-mirror pointing errors and global aberrations described above and normalized to match the data at the maximum intensity point. No other parameters were adjusted.

4. Implications for Čerenkov light imaging

Čerenkov light from a γ-ray initiated air shower aligned with the optic axis comes from a long, narrow cylinder of atmosphere. Since the cylinder of atmosphere is aligned with, but generally displaced from, the optic axis of the telescope, the image produced has a distinctive shape which is approximately elliptical with a major axis that points through the center of the telescope image plane and would extend through the core of the shower. Typical image shapes are shown in Hillas and Lamb (1987). These images differ from proton-initiated air shower images in two distinct ways : (1) the γ-ray images are narrower and (2) the major axis points toward the center of the image plane. The images initiated by protons are wider because of the larger transverse momentum characteristic of hadronic interactions and their orientations are random because the arrival directions are random. Hillas (1985) proposed using the rms spread of an image in the azimuthal direction on the camera focal plane (azwidth) as a γ/proton discriminant. The parameter is

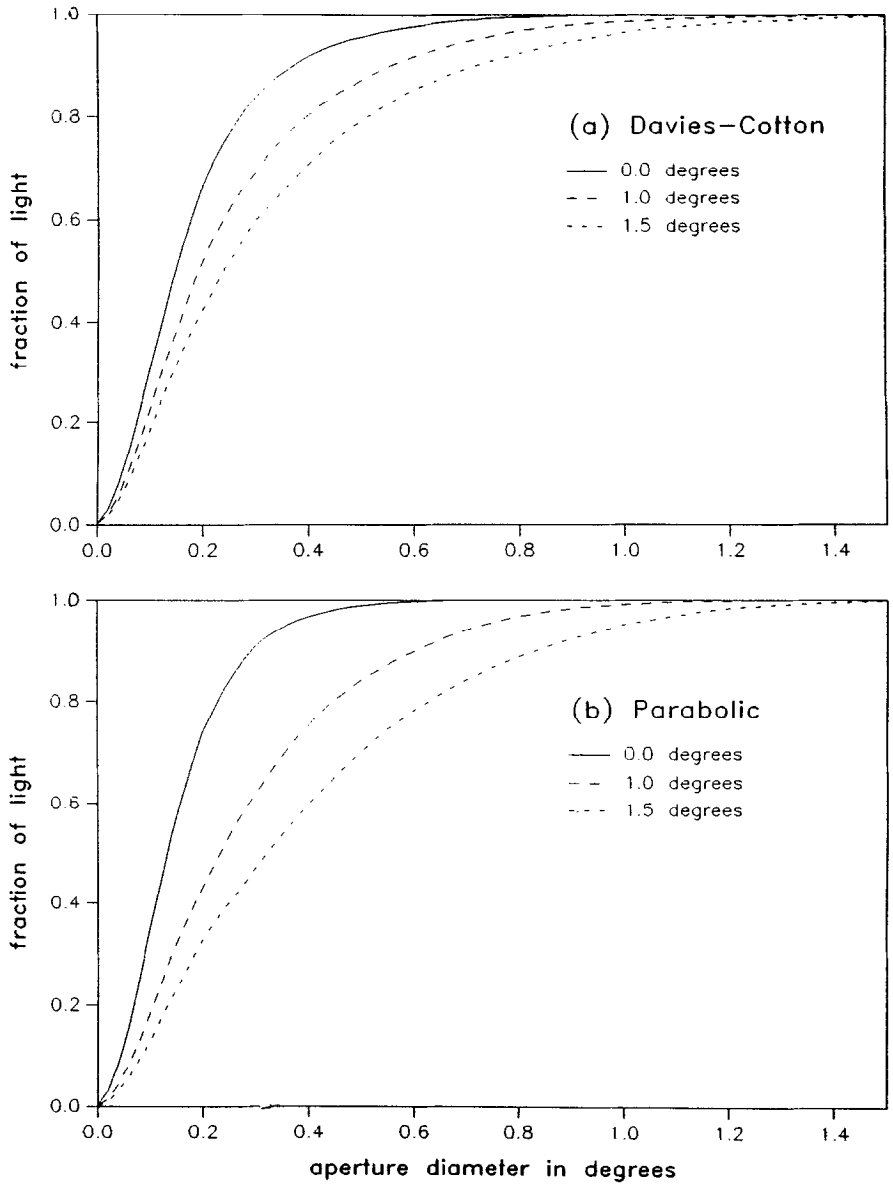

Fig. 5. Integral image shapes calculated for (a) the 10 m Davies-Cotton reflector and (b) a similar 10 m parabolic tessellated reflector are plotted above. The three curves for each reflector correspond to (*i*) a point source on the optic axis, (*ii*) a point source 1° off axis, and (*iii*) a point source 1.5° off axis. The abscissa is the diameter of a disk centered at the position the image would have with no aberrations, and the ordinate is the fraction of the total light that passes through this disk.

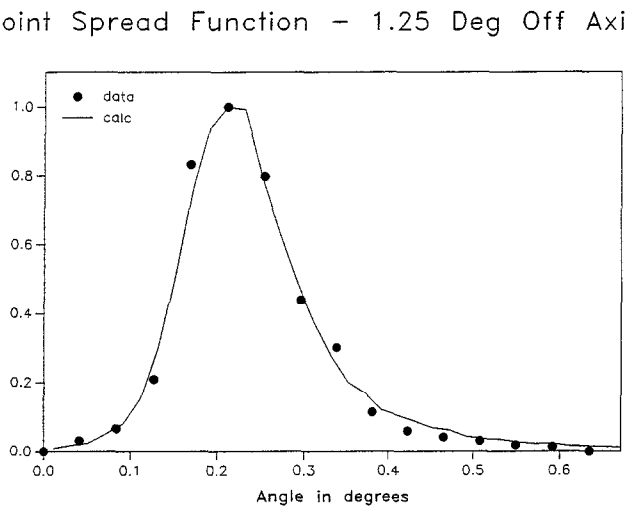

Fig. 6. A measured radial point spread function 1.25° off the optic axis is shown and compared with a solid curve calculated as described in the text.

sensitive to both the width and orientation of an image on the focal plane, with small values corresponding to the γ-ray domain. Detailed Monte Carlo simulations (Hillas 1985, Hillas and Lamb 1987) demonstrated the potential of this approach, which was realized in $9\,\sigma$ (Weekes et al. 1989) and $15\,\sigma$ (Lang et al. 1989) detections of TeV γ-rays from the Crab Nebula.

The success of the method obviously depends on the optical characteristics of the imaging camera. In order to quantify this, focal plane images have been computed using results from Monte Carlo simulations described in detail elsewhere (Macomb and Lamb 1990). The proton-initiated events were taken from an integral $E^{-1.65}$ spectrum and the γ-ray initiated events were taken from an integral $E^{-1.25}$ spectrum. Čerenkov photons from the simulations were mapped onto a photomultiplier tube matrix with a 0.25° pixel size corresponding to the present camera (Lewis et al. 1987, Cawley et al. 1990) in three ways : (a) with an ideal 10 m reflector with no aberrations, (b) with a Davies-Cotton 10 m reflector such as that presently used, and (c) with a standard parabolic 10 m reflector. Since the aberrations due to individual facets can, in principle, be made negligible by using a small facet size, global and facet aberrations were treated separately. In the simulations, events in which at least 2 of the inner 91 photomultiplier tubes detected a minimum of 40 photons were recorded (as described in detail in Cawley et al. 1990), resulting in about 200 recorded events for both γ's and protons. In this work azwidth distributions are used to quantify the quality of the telescope; the cases described the resulting azwidth distributions are shown in Fig. 7.

As can be seen from Fig. 7, the separation into γ and proton domains is maintained by both Davies-Cotton and parabolic shaped reflectors. In general azwidth

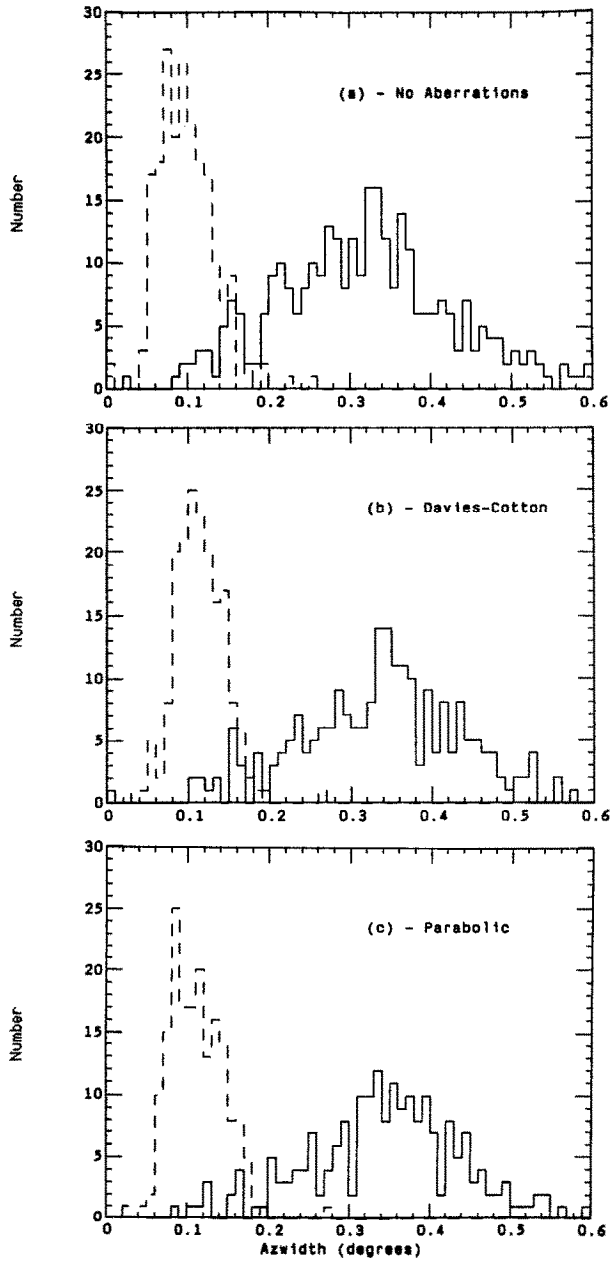

Fig. 7. Binned azwidth distributions for (a) aberration-free, (b) Davies-Cotton, and (c) parabolic reflectors are shown above for γ-ray initiated events (dashed) and proton initiated events (solid).

is increased by the inclusion of aberrations and the average values and standard deviations of the azwidth distributions are shown in Table 1. Although aberrations increase the average value of azwidth, they decrease the standard deviations. This is because narrower images tend to be spread out by a larger fraction than wide images. In a simple approximation, the intrinsic widths of the shower images add in quadrature with widths due to aberrations. It is clear from Table 1 and Fig. 7 that reflector rms widths due to aberrations should be kept less that 0.3°, and preferably comparable to 0.1°(or less). It is also apparent that an f/0.7 standard parabolic shape is completely acceptable for use in a Čerenkov imaging telescope, even though, as shown in the last section, the off-axis focusing characteristics are somewhat inferior to the Davies-Cotton design now in use. There is no evidence that its performance is inferior in the simulated azwidth distributions.

TABLE 1

Particle Case	γ $< azw >$	γ σ_{azw}	p $< azw >$	p σ_{azw}
no aberrations	.098	.036	.327	.122
Davies-Cotton	.113	.032	.343	.114
parabolic	.111	.035	.352	.111
facet	.129	.027	.329	.108

The last row in Table 1, labeled facet, shows the effects of including only facet and not global aberrations on the azwidth distributions. These were computed assuming an f/0.7 Davies-Cotton shape with 61 cm facet mirrors (the size presently used), although the results would be essentially the same for a parabolic shape. It is apparent that facet aberrations are significant in the present design and that they increase the intrinsic azwidth of γ-ray initiated showers from about 0.10° to about 0.13°. Assuming that the intrinsic shower widths and aberration widths add in quadrature and using the fact that the dominant facet aberration (astigmatism) scales linearly with facet mirror size, it follows that the facet mirror contribution to the azwidth values would be comparable to the global aberration contribution for 39 cm facets, i.e., the mean γ-ray azwidth value for facet aberrations would then be about 0.112°, the value for the global aberrations alone (Table 1).

It should be noted that Hillas (1989) has recently investigated the intrinsic accuracy with which arrival directions can be determined by using all available information in the Čerenkov light. The suprising result is 1–2 arcminutes. A 10 m mirror totally free of aberrations and a photoelectron detector with infinite resolution were assumed. In order to exploit this potential, an optical telescope of comparable

resolution (1–2 arcminutes) over a 4° field of view, and a light detector consisting of a very large number of photodetectors or perhaps a large image intensifier (as proposed by Mattox 1988) would be necessary. Simple, small f-number reflectors of the types considered here would not be adequate, even with very small facets, because of off-axis aberrations discussed in Sec. III.

In summary, although designed for focusing only on the optic axis, the spherical telescope design proposed by Davies and Cotton (1957) has good optical properties off the optic axis and is, in fact superior to a normal parabolic shape for off-axis images. Both designs are perfectly acceptable for Čerenkov imaging, and are well matched to focal plane detectors (Lewis et al. 1987; Cawley et al. 1990) consisting of closely packed photomultiplier tubes in both resolution and plate scale. Point spread functions with FWHM of less than 0.15° have been achieved over a 4° field of view for the present Davies-Cotton-design 10 m reflector. A disadvantage of the Davies-Cotton design is that light arriving at the focal plane from different portions of the telescope suffer different delays, i.e., the design is not isochronous. This broadens the time profile of the burst of Čerenkov light, requiring longer integration times which introduces additional night-sky noise into the images.

Acknowledgements

The author is indebted to D. J. Macomb for making available the results of his Monte Carlo simulations. He also thanks Tony Hayes for help with ray-tracing calculations and T.C. Weekes, G. Vacanti, M.J. Lang, M.F. Cawley, and R.C. Lamb for encouragement and useful suggestions. The work was supported, in part, by the U.S. Department of Energy.

References

Akerlof, C.W., Meyer, D.I., Lamb, R.C., Lewis, D.A., and Weekes, T.C. : 1989 in *SPIE Proc. EUV, X-ray, and Gamma-Ray Instrumentation for Astronomy and Atomic Physics,* **1159**, San Diego, California, 270.

Cawley, M.F., Fegan, D.J., Gibbs, K., Gorham, P.W., Hillas, A.M., Lamb, R.C., Liebing, D.F., MacKeown, P.K., Porter, N.A., Stenger, V.J., and Weekes, T.C. : 1985, in *Proc. 19th Internat. Cosmic Ray Conf.*, (La Jolla), **1**, 131.

Cawley, M.F., Fegan, D.J., Harris, K., Kwok, P.W., Hillas, A.M., Lamb, R.C., Lang, M.J., Lewis, D.A., Macomb, D., Porter, N.A., Reynolds, P.T., Schmid, D.J., Vacanti, G., Weekes, T.C. : 1990, *Experimental Astronomy*, in press.

Davies, J.M., and Cotton, E.S. : 1957 *Journ. of Solar Energy*, **1**, No. 2 and 3, 16-22.

Fegan, D.J., McBreen, B., O'Mongain, E., Porter, N.A., and Slevin, P.J. : 1968, *Canadian J. Phys.*, **46**, S433.

Fry, W.F. : 1986, in *Proc. NATO Advanced Workshop on VHE Gamma-Ray Astronomy*, (Publ. Reidel, Dordrecht), ed. K.E. Turver, 81.

Hill, D.A., and Porter, N.A. : 1961, *Nature*, **191**, 690.

Hillas, A.M. : 1985, in *Proc. 19th Internat. Cosmic Ray Conf.*, (La Jolla), **3**, 445.

Hillas, A.M., Lamb, R.C. : 1987 in *Proc. 20th Internat. Cosmic Ray Conf.*, (Moscow), **2**, 360.

Hillas, A.M. : 1989 in *Proc. of the Internat. Workshop on Very High Energy Gamma Ray Astronomy*, (Crimea, USSR), 136.

Lang, M.J., Cawley, M.F., Fegan, D.J., Hillas, A.M., Kwok, P., Lamb, R.C., Lewis, D.A., Macomb, D., Reynolds, P.T., Vacanti, G., and Weekes, T.C. : 1989 in *Proc. of the Workshop on the Physics and Experimental Techniques of High Energy Neutrino and VHE and UHE Gamma-Ray Particle Astrophysics,* Little Rock Arkansas, in press.

Lewis, D.A., Cawley, M.F., Fegan, D.J., Hillas, A.M., Kwok, P.W., Lamb, R.C., Reynolds, P.T., Porter, N.A., and Weekes, T.C. : 1987 in *Proc. 20th Internat. Cosmic Ray Conf.*, (Moscow), **2**, 360.

Macomb, D., Lamb, R.C., 1990 : in *Proc. of the 21'st Internat. Cosmic Ray Conf.*, (Adelaide), in press.

Mattox, J., 1988 : *Nucl. Instrum. Meth.*, **A271**, 652.

Resvanis, L. et al. : 1986, in *Proc. NATO Advanced Workshop on VHE Gamma-Ray Astronomy*, (Publ. Reidel, Dordrecht), ed. K.E. Turver, 225.

Rieke, G.H. : 1969 Ph. D. Thesis, Harvard University, unpublished; 1969 *Smithsonian Astrophysical Observatory Report* **301**, 1.

Smith, W.J. : 1966 *Modern Optical Engineering*, McGraw-Hill Book Co., New York.

Weekes, T.C. and Turver, K.E. : 1977, in *Proc. 12th Eslab Symposium*, Frascati, (ESA SP-124) 279.

Weekes, T.C. : 1988 *Physics Reports*, **160**, No. 1 and 2, 1-121.

Weekes, T.C. : 1988a, private communication.

Weekes, T.C., Cawley, M.F., Fegan, D.J., Gibbs K.G., Hillas, A.M., Kwok, P.W., Lamb, R.C., Lewis, D.A., Macomb, D., Porter, N.A., Reynolds, P.T., and Vacanti, G., : 1989 *Astrophys. Journ.*, 1989 .